

## An overview of responsive MRI contrast agents for molecular imaging

Byunghee Yoo<sup>1</sup>, Mark D. Pagel<sup>1</sup>

<sup>1</sup>Case Center for Imaging Research and Department of Biomedical Engineering, Case Western Reserve University, 10900 Euclid Ave. Cleveland, Ohio

### TABLE OF CONTENTS

1. Abstract
2. Introduction
3. MRI contrast mechanisms
4. Exogenous MRI contrast agents
5. Responsive MRI contrast agents
  - 5.1. Molecular imaging of proteins
    - 5.1.1. Contrast agents that bind to proteins
    - 5.1.2. Contrast agents that are catalyzed by enzymes
  - 5.2. Molecular imaging of nucleic acids
  - 5.3. Molecular imaging of metabolites
  - 5.4. Molecular imaging of oxygen
  - 5.5. Molecular imaging of metal ions
  - 5.6. Molecular imaging of pH
  - 5.7. Molecular imaging of temperature
6. Future Directions
7. Acknowledgements
8. References

## 1. ABSTRACT

This review focuses on MR contrast agents that are responsive to a change in physiological environment. The “response” mechanisms are dependent on 6 physicochemical phenomena, including the accessibility of water to the agent, rotational tumbling time, proton exchange rate, electron spin state, MR frequency, or local field inhomogeneities caused by the agent. These phenomena can be affected by the physiological environment, including changes in concentrations or activities of proteins, enzymes, nucleic acids, metabolites, oxygen and metal ions, and changes in pH and temperature. A total of 52 examples are presented, which demonstrate the variety and creativity of different approaches used to create responsive MRI contrast agents.

## 2. INTRODUCTION

During the last 30 years, Magnetic Resonance Imaging (MRI) has developed from an intriguing research project to an essential diagnostic method in the armamentarium of clinical radiologists. An estimated 26.6 million MRI examinations were performed annually in 2006, with a 3% annual increase in the number of MRI exams since 2003 (1). The growth of MRI is partly driven by the broad variety of clinical examinations that exploit many types of MRI contrast mechanisms in endogenous tissues. Different image contrast generated by different soft tissues can be used to assess anatomy at excellent spatial resolution that is typically approaches or exceeds 1 mm. Different image contrast can also assess physiological function, such as the function of the cardiopulmonary

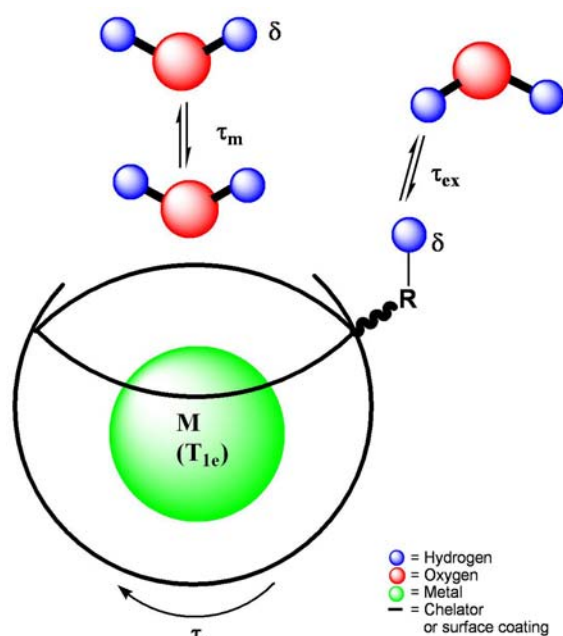


**Figure 1.** A schematic of responsive mechanisms for MR contrast agents. The water accessibility ( $\tau_m$ ), rotational tumbling time ( $\tau_r$ ), electron spin state ( $T_{1e}$ ), chemical exchange rate ( $\tau_{ex}$ ), and MR frequency ( $\delta$ ) are shown, but RF inhomogeneity is not shown in this scheme.

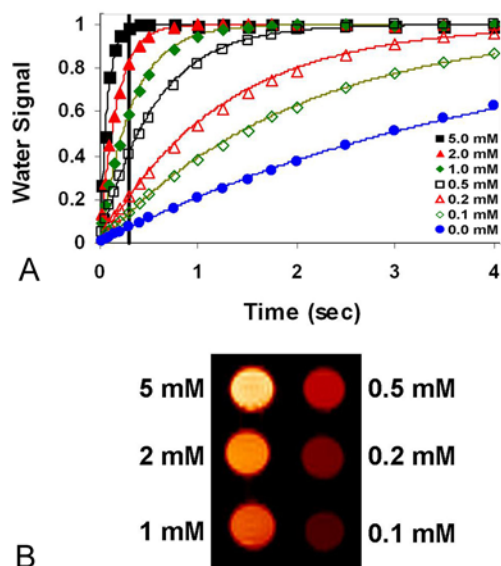


**Figure 2.** An example of a T1 MRI contrast agent. Solutions of GdDTPA were prepared at different concentrations and analyzed using a 9.4T (400 MHz) MR scanner at 37 degrees C. A) Magnetization recovers at different rates according to T1 relaxation times of different concentrations of Gd-DTPA. B) An MR image shows the effects of T1 relaxation on image contrast. The vertical line at 0.3 sec in graph A corresponds to the timing used to acquire the image. The 0 mM solution was not included in the image.

system (e.g., MR angiography of vasculature), neurological system (e.g., fMRI of brain activity), renal system (e.g., perfusion imaging of kidney function), musculoskeletal system (e.g., MR elastography of connective tissues), and cancer lesions (e.g., Dynamic Contrast Enhanced MRI of angiogenic tumors).

Although MRI contrast in endogenous tissues provides excellent sensitivity for detecting subtle changes in anatomy and function, MRI has poor specificity for attributing image contrast to pathologies. For example, MRI matches or surpasses X-ray mammography in its ability to identify breast cancer lesions, but MRI also detects many non-cancerous lesions that lead to erroneous false-positive diagnoses, so that MRI breast exams are currently only recommended for women with high cancer risk factors (2,3). In addition, the changes in anatomy or function that are detected with MRI are often the consequence of mid- to late-stage developments of the pathology, which are too late for the application of preventative or early-stage treatments. To meet these needs, MRI methods are being developed that cause changes in MR image contrast in response to molecular compositions and functions that serve as early biomarkers of pathologies. These new MRI methods comprise a major role in the paradigm of molecular imaging.

### 3. MRI CONTRAST MECHANISMS

A brief review of MRI contrast mechanisms is required in order to relate changes in MR image contrast to the response to molecular compositions and functions (Figure 1). The T1 relaxation time, also known as the time for longitudinal relaxation or spin-lattice relaxation, represents the time required for “relaxation” of “excited” magnetization to the thermal equilibrium state that is aligned with the main static field of the MRI magnet (typically considered to be the longitudinal direction; Figure 2). In order for T1 relaxation to occur, the magnetization must first be excited by absorbing radiofrequency (RF) energy, and then the absorbed energy must be released to the “lattice” of surrounding material through appropriate quantum-mechanical mechanisms. In the case of *in vivo*  $^1\text{H}$  MRI, the predominant mechanisms are dipole-dipole interactions between the hydrogen nucleus and another nucleus with a magnetic dipole that is rotationally tumbling at a rate that is sufficiently close to the same RF, and scalar interactions between a hydrogen nucleus that is in contact with an unpaired electron. Therefore, the T1 relaxation time can be changed in three ways: by altering the rotational tumbling time of a magnetic dipole, altering the accessibility of water to the dipole, or altering the electron spin state of the dipole.

The T2 relaxation time, also known as time for transverse or spin-spin relaxation, represents the loss of excited magnetization within the detection plane that is transverse to the main static field of the MRI magnet (Figure 3). This loss of magnetization from the transverse detection plane occurs as excited magnetization returns to equilibrium during the T1 relaxation time, so that the T2 relaxation time can be no slower than the T1 relaxation

## Responsive MRI contrast agents

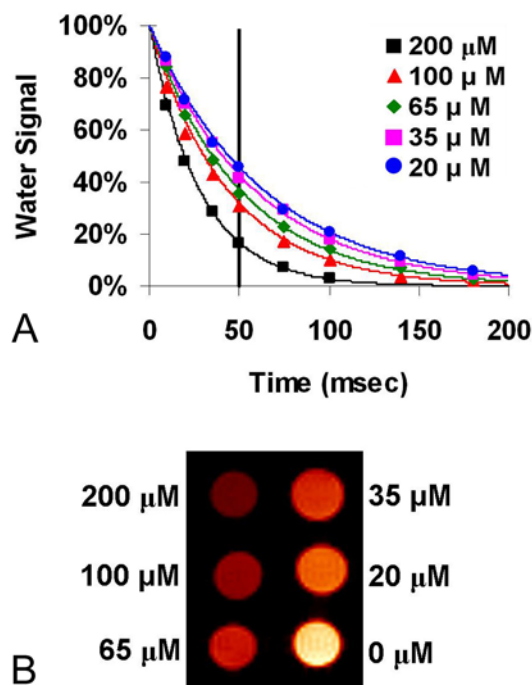


**Figure 3.** An example of a T2 MRI contrast agent. Solutions of dextran-coated iron oxide nanoparticles were prepared at different concentrations and analyzed using a 9.4T (400 MHz) MR scanner at 37 degrees C. A) Magnetization decays at different rates according to T2 relaxation times of different concentrations of the iron oxide. Due to the lengthy T2 relaxation time of the 0 micromolar solution, results from this solution are not included in the graph. B) An MR image shows the effects of T2 relaxation on image contrast. The vertical line at 50 msec in graph A corresponds to the timing used to acquire the image.

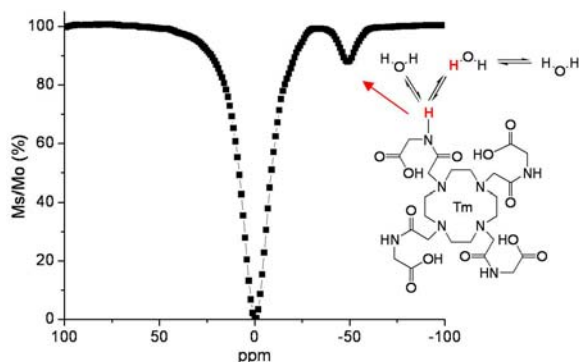


**Figure 4.** An example of a PARACEST MRI contrast agent. Tm-DOTAMGly (10mM in 5% D<sub>2</sub>O) was used to measure the PARACEST spectrum. A Varian Inova 600 MHz NMR spectrometer was used with a modified presaturation pulse sequence that included a continuous wave saturation pulse, saturation pulse power of 4.95 microTesla, saturation delay of 4 seconds and in 1 ppm increments from 100 ppm to -100 ppm.

time. Furthermore, the excited magnetization that is detected in the transverse plane represents a net sum of

very small magnetic moments from many nuclei, which must have the same MR frequency to produce a coherent net signal. Perturbations to nuclei that cause changes in MR frequency will cause a loss of coherence of among these very small magnetic moments, which contributes to the loss of the net coherent magnetization from the transverse detection plane. These perturbations arise from a “spin-spin” exchange of energy between two dipolar hydrogen nuclei, which become more efficient as the rotational tumbling time of the two nuclei becomes slower. These perturbations also arise from spatial inhomogeneities in the main magnetic field that cause differences in MR frequencies from hydrogen nuclei in different tissue locations but are otherwise in homogenous environments (the inclusion of this type of transverse relaxation is often termed T2\* relaxation). Therefore, the T2\* relaxation time can be changed in two ways: by altering the rotational tumbling time of a magnetic dipole, or by altering the local inhomogeneities in the main magnetic field.

A fundamentally new type of exogenous MRI contrast agent can be detected through the mechanism of Chemical Exchange Saturation Transfer (CEST; Figure 4). These contrast agents contain hydrogens that undergo chemical exchange with hydrogens of surrounding water molecules. These hydrogens may lie within functional groups in the covalent structure of the contrast agent, such as amide, amine, or hydroxyl groups. These hydrogens may also be part of a water molecule that is noncovalently bound to the metal for a relatively long lifetime, so that the water molecule is effectively part of the structure of the contrast agent for a transient period. Selective saturation can be applied at the specific MR frequency of the exchangeable hydrogens, which reduces the detectable magnetization from these hydrogens. Rapid chemical exchange with water causes a transfer of reduced detectable magnetization that contributes to the water signal. The chemical exchange rate must be slower than the difference in MR frequency between the hydrogen on the contrast agent and the hydrogen on a water molecule, so that the hydrogens have magnetically distinct frequencies that can allow for selective saturation of the agent’s MR frequency to generate a CEST effect. Continuous selective saturation and chemical exchange enhances the CEST effect, providing improved MRI sensitivity of the agent. Therefore, CEST can be changed in two ways: by altering the MR frequency of the hydrogens that exchange with water, or by altering the hydrogen exchange rate with water.

## 4. EXOGENOUS MRI CONTRAST AGENTS

Most molecular imaging studies critically depend on the development of exogenous agents that change image contrast in response to molecular compositions or functions within *in vivo* tissues. Exogenous T1 relaxation agents typically contain Gadolinium, which has a large spin-7/2 magnetic dipole moment and seven unpaired electrons, and therefore has excellent characteristics to decrease the T1 relaxation time of water molecules that are near the Gadolinium metal ion. Exogenous T2\* relaxation agents typically contain iron oxide nanoparticles that are

## Responsive MRI contrast agents

superparamagnetic and cause local magnetic field inhomogeneities that decrease the  $T_2^*$  relaxation time of water molecules that are near the iron oxide nanoparticle. Exogenous CEST agents typically contain paramagnetic lanthanide ions other than Gadolinium, which shift the MR frequencies of a CEST agent's hydrogen nuclei. Large frequency shifts of these PARAMagnetic CEST (PARACEST) agents greatly facilitate selective excitation and also allow for faster hydrogen exchange rates with water that improve detection sensitivity.

Many exogenous MRI contrast agents are designed to bind to endogenous molecules in a reversible manner that only involves non-covalent interactions, such as peptides that bind to cell receptors or extracellular matrix components. Reversible responsive MRI contrast agents can change their  $T_1$  relaxation time upon binding to their target molecule, by increasing their rotational tumbling time or water accessibility, or by changing the electron spin state of the agent. Similarly, the non-covalent binding of many small iron oxide nanoparticles to a molecular target can create a larger superparamagnetic nanoparticle, which increases local magnetic field inhomogeneities and decreases  $T_2^*$  relaxation times. A PARACEST agent can show an altered chemical shift or hydrogen exchange rate after non-covalent binding to a target molecule.

Exogenous MRI contrast agents are relatively insensitive, requiring a minimum threshold of 0.01-10 mM for adequate detection during *in vivo* applications. Endogenous metabolites that are present at concentrations that are higher than the detection threshold are feasible targets for this approach. Nucleic acids are typically present at concentrations of 1-1,000 pM, and intracellular proteins are typically present at concentrations of 1 to 1,000 nM, and therefore these reversible responsive agents have been difficult to use to target intracellular proteins and nucleic acids. For comparison, *in vivo* PET, SPECT, and fluorescence imaging contrast agents typically have detection sensitivity thresholds of picomolar concentrations and are more practical for detecting intracellular proteins and nucleic acids through a reversible binding mechanism. Extracellular proteins can exist at typical concentrations of 10-10,000 nM, so that the most abundant proteins may possibly serve as targets for reversibly-binding MRI contrast agents. Newer approaches that load MRI contrast agents onto nanoparticles may overcome this sensitivity problem, but at the expense of altered pharmacokinetics and potential toxicities. In addition, the specificity of the non-covalent binding for the desired target molecule relative to other potential targets must be carefully evaluated, in order to confidently interpret the response of the reversible MRI contrast agent.

Alternatively, responsive MRI contrast agents may be designed to undergo irreversible covalent changes during interactions with endogenous molecules, such as agents that are substrates for enzymes. The  $T_1$  relaxation time of an irreversible responsive MRI contrast agent can be changed through enzymatic cleavage of a ligand that blocks water accessibility to the agent's metal ions. These

MRI contrast agents can change their  $T_1$  or  $T_2^*$  relaxation times by undergoing enzymatic polymerization or depolymerization that changes the agent's rotational tumbling time. Polymerization or depolymerization can also alter the association of small iron oxide nanoparticles that form a larger superparamagnetic nanoparticle. PARACEST agents can undergo covalent changes that change chemical functional groups, which exhibit altered hydrogen exchange rates and MR frequencies of the exchangeable hydrogens in the functional group. Irreversible responsive contrast agents can exploit a high catalytic turnover rate from a relatively low concentration of target enzyme to generate a high concentration of responsive agent that is above the MRI detection threshold. The high specificity of the enzyme reaction may also lend confidence when interpreting the response of an irreversible MRI contrast agent.

In order to translate changes in image contrast to these changes in  $T_1$  relaxation time,  $T_2^*$  relaxation time, or the PARACEST effect, other characteristics that change image contrast must be constant or monitored by other methods. In particular, the concentration of the contrast agent affects image contrast, and *in vivo* pharmacokinetics rarely allow for constant tissue concentrations of contrast agents during the MRI scan session, so that the concentration of the contrast agent must be monitored. This may be accomplished by adding a second, unresponsive contrast agent that has identical pharmacokinetics or that is covalently linked to the responsive contrast agent. This poses a daunting problem for MRI contrast agents that depend on  $T_1$  and  $T_2^*$  relaxation times, because the  $T_1$  or  $T_2^*$  contrast in a MR image can only monitor one agent during the MRI scan session, and the two types of relaxation times are too correlated to distinguish one effect from the other during the same MRI scan session. The addition of a second, unresponsive contrast agent during the same scan session is feasible with PARACEST MRI, because PARACEST agents can be selectively detected via different saturation frequencies.

## 5. RESPONSIVE MRI CONTRAST AGENTS

### 5.1. Molecular imaging of proteins

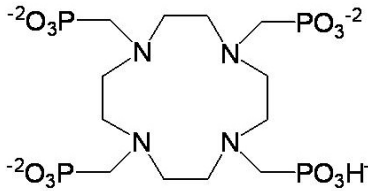
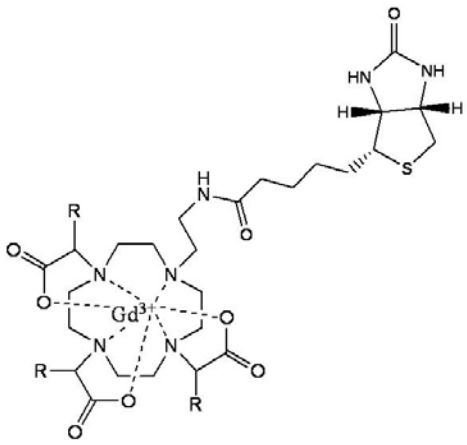
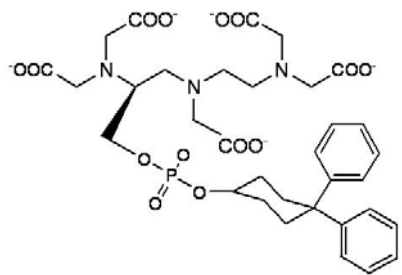
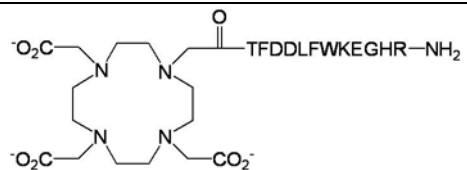
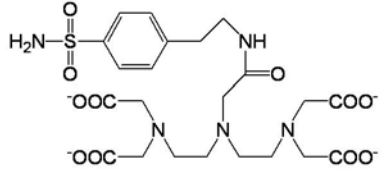
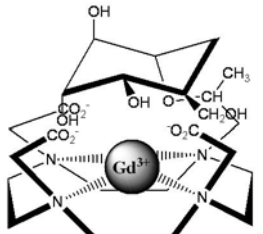
Proteins are responsible for a broad variety of molecular compositions and functions, and therefore serve as excellent biomarkers for many pathologies. The current human proteome consists of 21,688 known proteins (4,5) and approximately 600 to 1500 of these proteins are considered to be molecular targets of potential drug therapies. Responsive MRI contrast agents provide a tremendous opportunity to evaluate the human proteome and protein-targeting chemotherapies in an *in vivo* context (Table 1).

#### 5.1.1. Contrast agents that bind to proteins

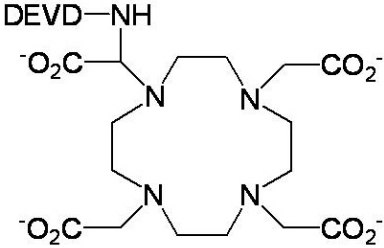
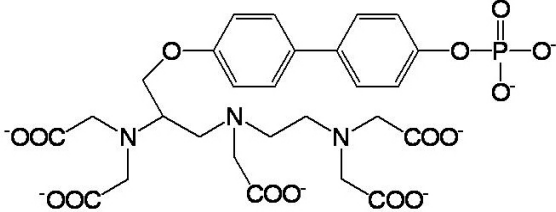
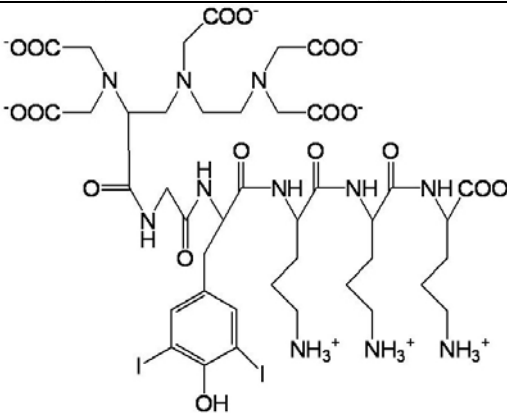
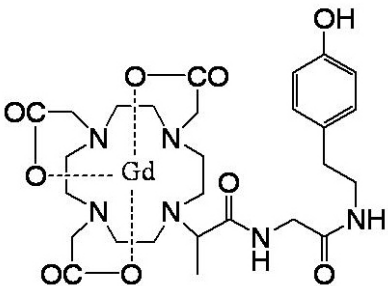
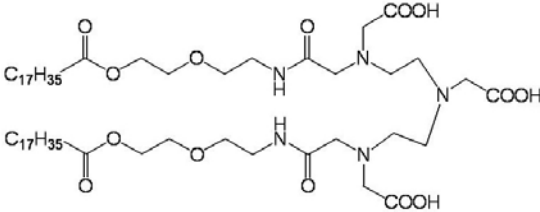
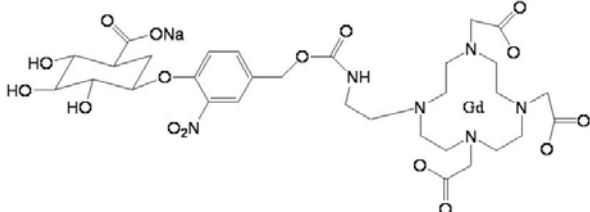
Due to the relative insensitivity of MRI, responsive contrast agents are generally limited to targeting proteins that are present at high concentrations, such as proteins that contribute to connective tissues and proteins that reside in the blood pool at high concentrations. For

## Responsive MRI contrast agents

**Table 1.** Structures of MR contrast agents responsive to proteins

Responsive to	Structure	References
Hydroxyapatite		6
Avidin		7
Human serum albumin		8
Gal80		9
Carbonic anhydrase		10
Beta-galactosidase		12

**Responsive MRI contrast agents**

Caspase-3		13
Alkaline phosphatase		14
Human serum albumin		15
Peroxidase		17
Esterase		21
Glucuronidase		22

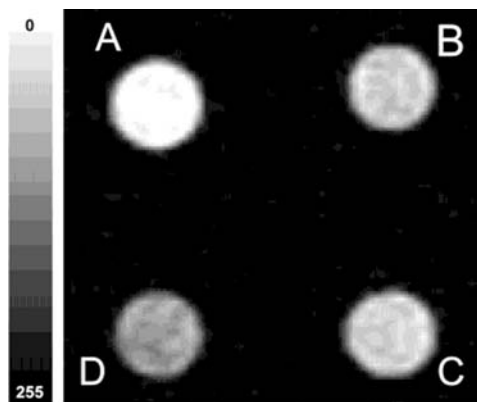


**Figure 5.** An example of a protein-responsive MRI contrast agent. T1-weighted MR images of a contrast agent shows preferential binding to the Gal80 protein. Four tubes (3 mm OD) containing 14 micromolar  $\text{Gd}^{3+}$ -G80BP plus (A) 11 micromolar Gal80, (B) 11 micromolar BSA, and (C) no protein. Sample D contained only buffer. Images were collected at room temperature with a Philips 1.5T Clinical Imager using the body coil as transmitter and a knee coil as receiver. A single 4 mm slice was acquired centered at the sample height (15 mm). The FOV was 50 x 50 mm and the matrix size was 256 x 256 points. A standard clinical T1-weighted spin echo image sequence with TR/TE 300/16 ms and two averages were used. Reproduced with permission from (9).

example, a phosphonated Gd chelate,  $\text{GdDOTP}^{5-}$ , is designed to bind to hydroxyapatite, which reduces water accessibility and increases the T1 relaxation time of the agent (6). Hydroxyapatite is a major component of healthy bone tissue, so that this agent can be used to bone lesions that are devoid of hydroxyapatite. As another example, the rotational tumbling time of a biotinylated contrast agent, DO3A-EA, is increased when bound to the larger avidin protein that is administered to the patient, so that the MRI contrast responds to high concentrations of avidin in the cardiovascular system (7). Similarly, another contrast agent, MS-325, binds to human serum albumin (HSA) that resides in the blood pool at high concentration, which increases the tumbling time of the contrast agent upon binding to this larger protein (8). A contrast agent with a peptidyl ligand has been designed to bind to the Gal80 glucose storage protein, which also increases the tumbling time of the agent (9; Figure 5). Carbonic anhydrase has been selectively targeted by Gd-DTPA-sulfonamide ethylene sulfanilamide, which has a long tumbling time after binding to its protein target (10). The longer tumbling times lead to decreased T1 relaxation times for each agent when bound to the target protein. For each of these cases, care must be taken to ensure that each binding agent is specific to the intended protein target.

Other examples have shown that antibodies and peptides that are labeled with MRI contrast agents can bind overexpressed protein cell receptors that are present at high concentrations. Although some examples are promising candidates for detecting these cell receptors, the MRI

contrast is dependent on the accumulation of the agent, and not a response caused by a change in physical properties of the agent. Protein targeting with unresponsive MRI contrast agents has been the subject of another excellent review (11), and will not be repeated in this review of responsive contrast agents.

### 5.1.2. Contrast agents that are catalyzed by enzymes

The targeting of enzymes provides several important advantages for the design of responsive MRI contrast agents. First, the high catalytic rate of a relatively low concentration of enzyme can develop a relatively high concentration of altered contrast agent, so that poor MRI sensitivity is less problematic for enzyme detection. Second, the specificity of enzymatic reactions is usually high, so that a change in MRI contrast can often be confidently attributed to the specific targeted enzyme. Lastly, enzymatic activity can cause a variety of irreversible responses in a contrast agent, which can be exploited to develop many types of responsive MRI contrast agents.

One of the seminal examples of a responsive MRI contrast agent exploits a change in water accessibility after beta-galactosidase enzymatically cleaves a galactopyranose ligand from the contrast agent (12). More recently, the hydrogen exchange rate and MR frequency of a PARACEST agent have been shown to be altered after a peptidyl ligand of the agent is cleaved by caspase-3 (13; Figure 6). Only 4.3 micromolar and 3.4 nanomolar concentrations of each respective enzyme was required to generate sufficient MRI contrast in a practical time frame, and the specificity for each respective contrast agent substrate was shown to be excellent. The rotational tumbling time can be changed after a phosphate monoester ligand of a contrast agent is hydrolyzed to an alcohol by alkaline phosphatase, which can then more easily bind to HSA (14). Similarly, a lysine-containing ligand of a contrast agent can be cleaved by thrombin-activatable fibrinolysis inhibitor, which facilitates interactions between the contrast agent and HSA and causes an increase in rotational tumbling time (15).

The rotational tumbling time of a contrast agent can be changed by polymerizing monomeric agents. Polymerization of phenolic contrast agents has been exploited to detect several peroxidases (16), including myeloperoxidase and oxidoreductase (17-20). The increase in tumbling time caused by the polymerization is sufficient to cause a three-fold decrease in T1 relaxation time. The polymerization also aids in retaining the contrast agent at the target site, either through slower pharmacokinetics of the polymeric form of the agent, or by cross-linking the agent to the local extracellular matrix. As another example, a stearic acid ligand of a contrast agent can be cleaved by an esterase, which leads to spontaneous polymerization of the cleaved chelate (21).

Degradation of a polymer can also change the rotational tumbling time of a contrast agent. This mechanism is typically exploited by conjugating contrast agents with a linker that is cleaved by a specific enzyme.



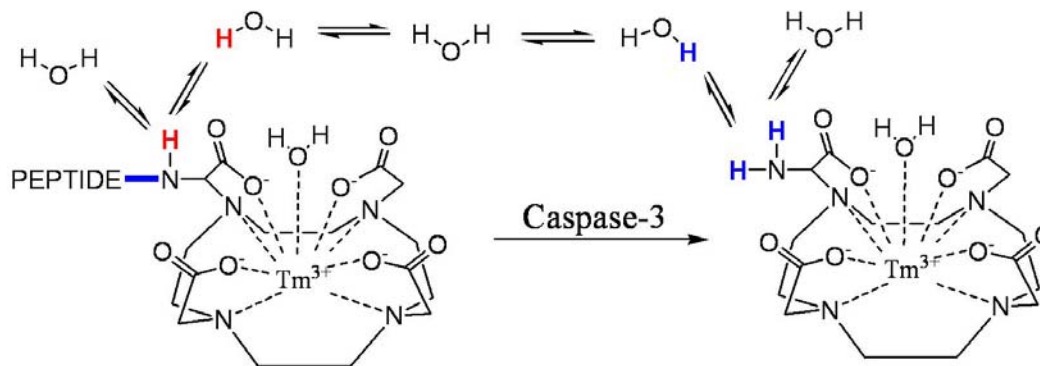


**Figure 6.** An example of an enzyme responsive MRI contrast agent. Caspase-3 cleaves the amide bond at the end of specific peptide sequence, DEVD, to convert an amide bond to an amine group. The amide proton and amine protons show different MR chemical shifts, which can be detected with PARACEST MRI.

For example, a glucuronide linker is cleaved by glucuronidase (22), and a hyaluronan linker is cleaved by hyaluronidase (23,24), which releases the Gadolinium chelate from the polymer. The relatively rapid pharmacokinetics of monomeric contrast agents can accelerate removal of the agent from the site of degradation, which can further enhance the response of the agent to degradative enzyme activity.

Polymerization or degradation can also be exploited to change the association of iron oxide nanoparticles that cause local field inhomogeneities, which has been termed as a 'magnetic relaxation switch'. Peroxidase-induced polymerization of phenolic contrast agents can assemble dextran-coated iron oxide nanoparticles to create an even stronger superparamagnetic particle that decreases the  $T_2^*$  relaxation time (25). Caspase-3-induced degradation (26) or MMP-2-induced degradation (27) of a short peptide sequence that links multiple avidin-biotin- $T_2^*$  contrast agents can increase the  $T_2^*$  relaxation time. Degradation of a double-stranded DNA linker by DNA methylation & cleavage enzymes can also cause an increase in  $T_2^*$  relaxation time (28).

## 5.2. Molecular imaging of nucleic acids

The genomics revolution has identified an abundance of nucleic acid targets among ~24,000 human genes that are potential biomarkers of pathologies (29,30). The strong interactions between complementary nucleic acid sequences can provide very high selectivity for detecting a specific nucleic acid target. The 'magnetic relaxation switch' method has been successfully applied to detect the DNA sequence for Green Fluorescence Protein in biochemical solutions within well plates, versus DNA sequences with single mismatches relative to the target DNA sequence (26; Figure 7). As another example, A DNA-binding protein that is conjugated to a peptide-based  $Gd^{3+}$ -chelator can change  $T_1$  relaxation time in response to DNA concentration (31). This method exploits the aggregation of iron oxide-labeled nucleic acid sequences that bind to a portion of the target DNA sequence, which increases local field inhomogeneities and decreases  $T_2^*$  relaxation times. Yet directly detecting a specific nucleic acid sequence within the *in vitro* or *in vivo* context is a

daunting challenge for MRI, primarily due to the extremely low concentration of specific DNA and RNA sequences that are present at ~1 and 10-100 copies within each cell, respectively. The intranuclear and intracellular locations of nucleic acids pose the additional problem of intracellular delivery and trafficking of the nucleic acid-targeting contrast agent.

A more promising approach is the use of a reporter gene imaging strategy to study gene expression during *in vitro* or *in vivo* studies (32,33). This strategy requires transgenic manipulation of the cell or animal model to include two genes that are co-expressed. One of the genes is the 'target gene' that is the focus of the gene expression study. The other gene represents the 'reporter gene' that encodes for a 'reporter protein' that can be detected by a responsive MRI contrast agent using one of the many mechanisms discussed in section 5.1. A responsive MRI contrast change reports on the expression of the 'target gene'. Reporter gene imaging with optical and nuclear imaging modalities has become tremendously successful, and similar successes with MRI reporter gene strategies are likely to emerge in the near future.

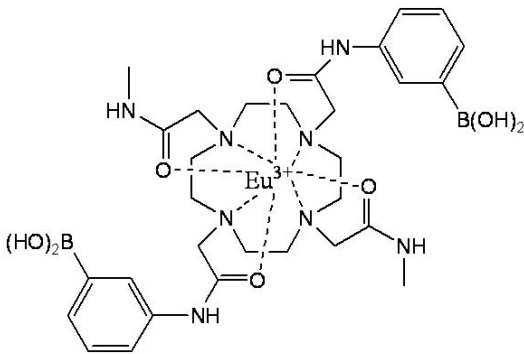
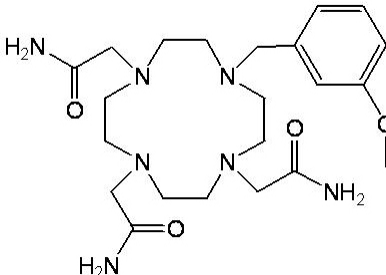
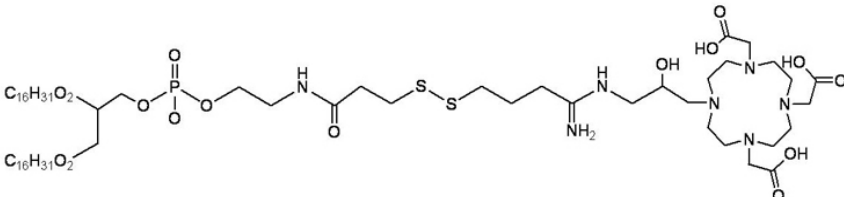
## 5.3. Molecular imaging of metabolites

Many metabolites exist at high concentrations within an *in vitro* or *in vivo* environment, which greatly facilitates their detection by responsive MRI contrast agents. The variety of molecular structures provides opportunities to exploit several mechanisms that are employed by responsive MRI contrast agents (Table 2). Yet this variety of molecular structures is a challenge when designing responsive MRI contrast agents, so that first-generation agents may only weakly interact with the target metabolite. In addition, care must be taken to selectively detect one of many similar metabolites to ensure that the MRI response can be attributed to the target metabolite.

PARACEST agents are insensitive and require high concentrations of their target, but can be very responsive to weak interactions. Therefore, PARACEST agents are well suited for the detection of metabolites that are present at high concentrations. The hydrogen exchange rate of a PARACEST contrast agent has been shown to



**Table 2.** Structures of MR contrast agents responsive to metabolites

Responsive to	Structure	References
Glucose		34
Lactate		36
Free radical		38

change when the agent noncovalently binds to a sugar, although selectivity for specific sugars is marginal (34,35; Figure 8). The MR frequency of another PARACEST contrast agent changes from -29.1 ppm to -15.5 ppm when the agent noncovalently binds to L-lactate (36). Both the hydrogen exchange rate and the MR frequency of a PARACEST contrast agent change when the agent undergoes an irreversible covalent reaction with nitric oxide (Liu, Li, and Pagel, unpublished results). In each case, care must be taken to ensure that the interactions between high concentrations of the PARACEST agent and the metabolite do not perturb the biological system.

Fewer mechanisms have been exploited to change T1 or T2\* relaxation times in response to metabolites. Water accessibility can be altered when glucose binds to a Gadolinium chelate (37). Degradation of thiol-containing polymeric contrast agents can be caused by dithiothreitol or primary radicals OH•, H•, HO2•, H3O+, O2•-, or e•-aq (38). Further research to improve the strength of interactions between contrast agents and specific metabolites is required to exploit additional responses in T1 or T2\* relaxation times.

#### 5.4. Molecular imaging of oxygen

The partial pressure of oxygen, pO<sub>2</sub>, is relevant to many pathologies including cerebral infarcts and tumor

tissues (39,40). The oxidation state of many metal ions is dependent on pO<sub>2</sub>, which can be exploited to change the response of MRI contrast agents relative to pO<sub>2</sub>. Manganese complexes of 5,10,15,20-tetrakis-(p-sulfonatophenyl) porphinate (tpps) change their redox state between Mn<sup>II</sup> and Mn<sup>III</sup> depending on pO<sub>2</sub>. The T1 relaxation time of the Mn<sup>III</sup> complex is mainly affected by the electronic relaxation time and that of the Mn<sup>II</sup> complex is mainly controlled by the rotational motion of the complex (41). The iron in the porphyrin ring of hemoglobin changes in redox state from diamagnetic Fe<sup>II</sup> to paramagnetic Fe<sup>III</sup> when bound to oxygen. The injection of 2~5 microliters of 8 mM of hemoglobin can show significant pO<sub>2</sub>-dependent changes in the contrast of T2-weighted MR images (42; Figure 9).

In addition to a change in electron spin state, the rotational tumbling time can also be changed in response to pO<sub>2</sub>. The boronic functionalities of Bis(*m*-boroxyphenylamide)-(Gd-DTPA) bind to fructosamine on the glycated surface of oxygenated hemoglobin, but have less affinity for binding deoxygenated hemoglobin (43). The increase in rotational tumbling time upon binding causes a decrease in T1 relaxation time. Although these responsive MRI contrast agents show promise, these agents must be designed to measure physiologically relevant ranges of pO<sub>2</sub>.

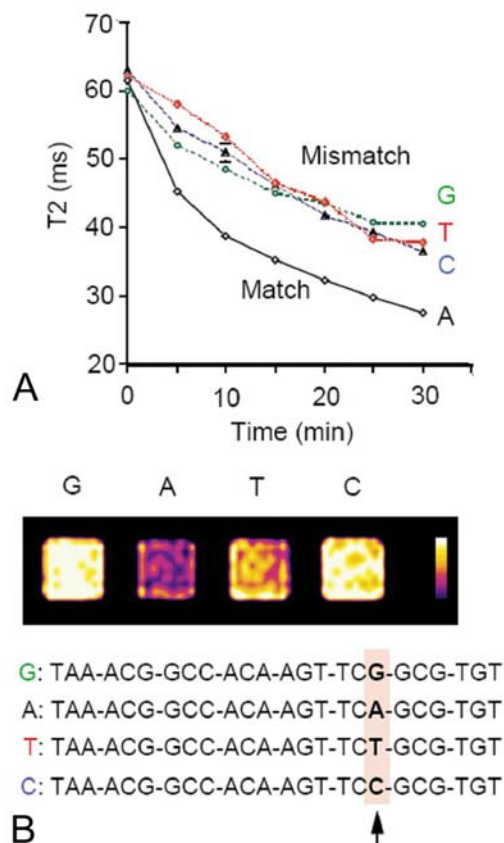


**Figure 7.** An example of a DNA-responsive MRI contrast agent. The contrast agent consisted of a complimentary oligonucleotide conjugated to an iron oxide nanoparticle (10 microgram Fe/ml). This agent was added to solutions of the target oligonucleotide (containing A) and other solutions of oligonucleotides containing single-nucleotide mismatches G, T, and C (53 fmol) in 25 mM KCl, 50 mM Tris-HCl, pH 7.4. The perfect target sequence is clearly distinguished from single-nucleotide mismatches by benchtop measurements of the temporal changes in T2 relaxation times (A) and T2 weighted MRI (B) of samples. Reproduced with permission from (26).

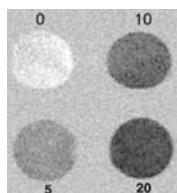


**Figure 8.** An example of a metabolite-responsive MRI contrast agent. PARACEST images of phantoms containing a glucose responsive MRI contrast agent and either 0, 5, 10, or 20 mM glucose are measured in PIPES (100 mM) buffer at pH 7.0. The image parameters were as follows: TR/TE ) 3000/18 ms, FOV = 40 x 40 mm, thickness 2 mm, data matrix 256 x 256, saturation duration time of 2 s at a power of 1020 Hz at a frequency offset of 50 and 30 ppm. The PARACEST image was obtained by subtracting pixel by pixel the image at 50 ppm from that at 30 ppm. Reproduced with permission from (34).

### 5.5. Molecular imaging of metal ions

Metal ions, especially divalent metal ions, are associated with many biological signaling pathways and pathologies. The rapid flux of metal ions on a sub-second time scale can require rapid measurements, which can pose a particular challenge for accurate quantification through MRI contrast changes. As with  $pO_2$  measurements, the measurements of metal ion concentrations must be conducted in physiologically relevant concentration ranges. Consideration should also be given for ensuring that the MRI contrast agent detects the desired metal, although metal binding motifs often show excellent specificity for one type of metal.

Chelates that bind metals are often incorporated into contrast agents to change MRI contrast in response to metal concentrations (Table 3). For example, calcium can be chelated by four carboxylates to form a complex with an association constant of approximately 960 nM. A calcium-responsive MRI contrast agent has been designed with two Gd-DOTA moieties linked by a bis-anilide bridge that contains four carboxylates (44,45). When calcium is absent, the carboxylates bind to the Gadolinium ions, which inhibit water accessibility and increases T1 relaxation time. Similarly, carboxylate ligands of  $N,N,N',N'$ -tetrakis(2-pyridylmethyl)ethylenediamine (TPEN) readily complex with  $Zn^{2+}$ , but bind to Gadolinium in the absence of  $Zn^{2+}$  (46,47). Iron-responsive MRI contrast agents with a phenanthroline-like chelator moiety have been used to create tris complexes (48) or trinuclear structures (49) that have increased rotational tumbling times and decreased T2\* relaxation times. Another iron-responsive MRI contrast agent has a 2,2'-bipyridine moiety that binds to  $Fe^{2+}$  ions and then self-assembles into a metallostar  $[Fe\{Gd_2L(H_2O)_4\}_3]^{4+}$  structure that has a longer rotational tumbling time (50). A zinc-responsive MRI contrast agent with pyridine donors shows a faster hydrogen exchange rate and improved PARACEST when the pyridines chelate zinc. The chelation causes a subtle conformational change from a square-antiprism (SAP) geometry to a twisted-square-antiprism (TSAP) geometry, which facilitates the exchange of bulk water with the water molecule directly bound to the lanthanide of the agent (51). In general, these examples lack information regarding the association constants and of the metal complexation, which is required to understand whether these agents can measure a relevant range of physiological metal concentrations for particular biomedical applications.

Proteins and peptides can reversibly associate with metals to trigger intermolecular associations. This biochemical mechanism has been exploited to generate aggregates of iron-labeled calmodulin and iron-labeled M13 peptide in the presence of calcium, with a subsequent decrease in T2\* relaxation time (52; Figure 10). This example shows the potential creativity in exploiting mechanisms in biochemistry and molecular biology as additional steps to change MRI contrast in response to molecular biomarkers.

### 5.6. Molecular imaging of pH

Assessments of altered pH can be used to diagnose the progression of many pathologies, including

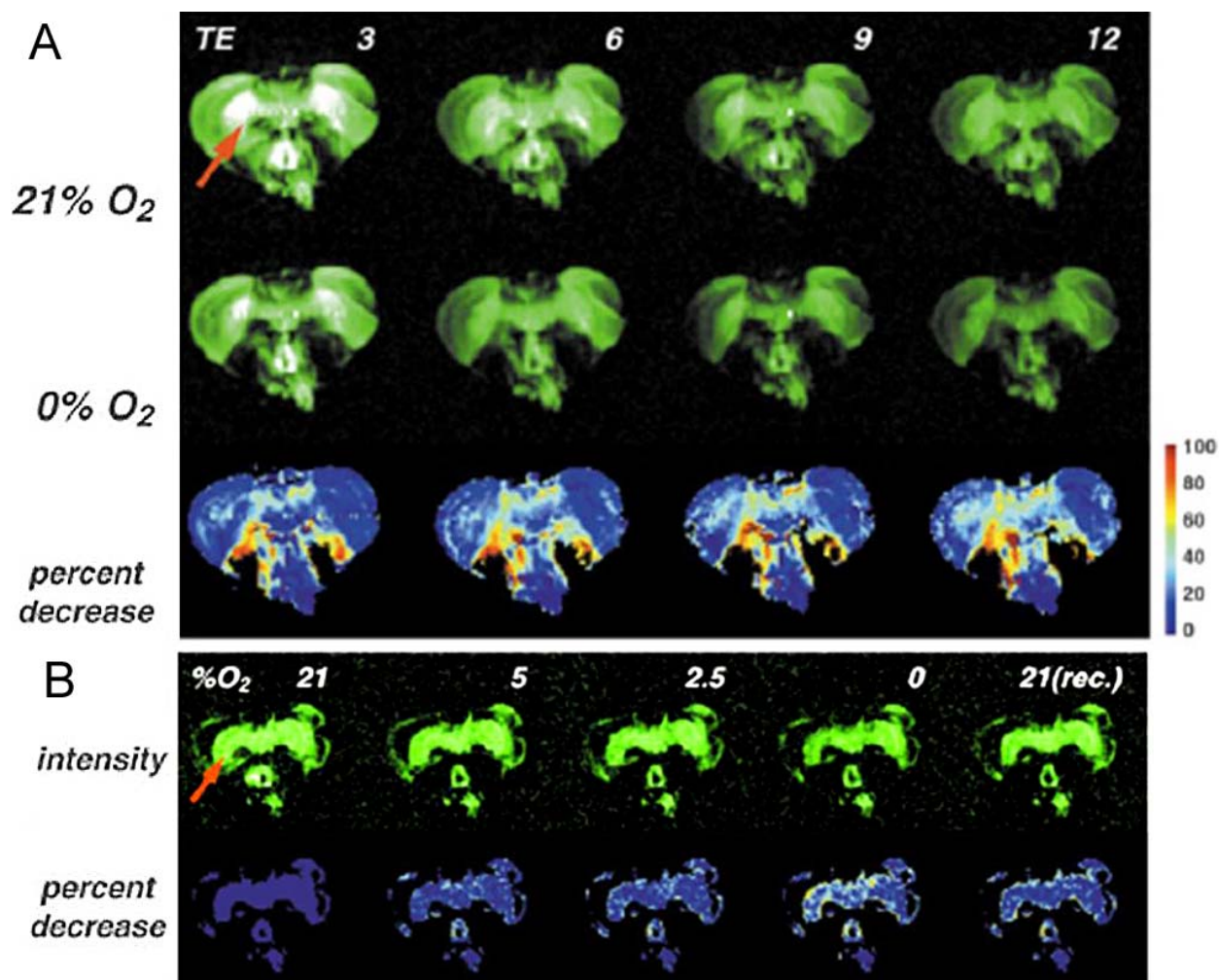


**Figure 9.** An example of a pO<sub>2</sub>-responsive MRI contrast agent. The T2-weighted MRI signal decreases with TE and O<sub>2</sub> depletion in xHb-injected fly brains. Reproduced with permission from (42).

renal failure, ischemia, and chronic obstructive pulmonary disease, and can also be critical for developing therapies that are effective in tissue environments with altered pH (53). Measuring altered pH is particularly relevant for cancer assessments, because poor perfusion, increased lactic acid secretion, and reduced bicarbonate levels within tumor tissues can create high H<sup>+</sup> concentrations within the interstitial fluid (54). MRI of pH-responsive contrast agents (Table 4) is particularly well suited for evaluating pH variations over small tissue volumes due to its high spatial resolution.

The ideal pH-responsive agent should accurately measure the entire physiological pH range from 6.0 to 8.0 through a monotonic change in T1 relaxation time, T2\* relaxation time, or PARACEST. The concentration of these pH-responsive agents must be taken into account to assign image contrast to pH values. A pH-unresponsive contrast agent can be used to account for concentration of the pH-responsive agent (55,56). Two T1 or T2\* contrast agents must be serially administered, but two PARACEST contrast agents can be selectively detected so that

simultaneous administration of two PARACEST contrast agents may be feasible.

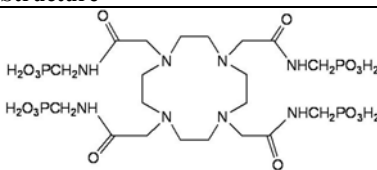
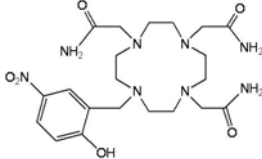
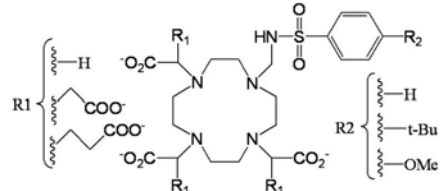
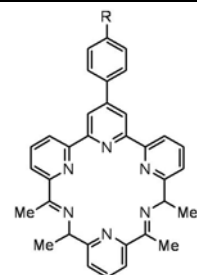
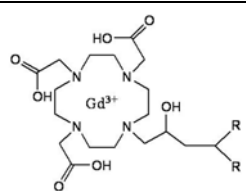
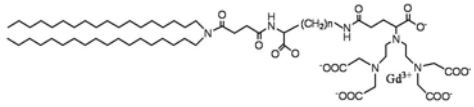
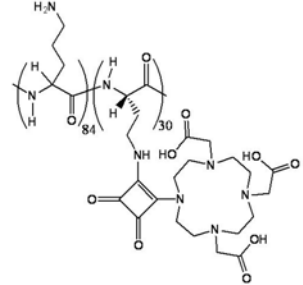
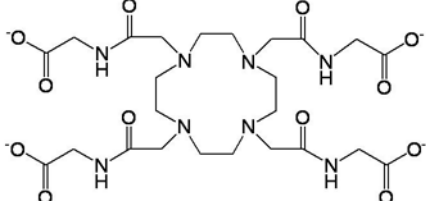
MRI contrast agents can include pH-dependent ligands that alter water accessibilities. Gd<sup>3+</sup>-DOTA-tetraamide phosphonate (Gd(DOTA)-4AmP<sup>5-</sup>) shows a two-fold increase in T1 relaxation time from pH 6.0 to 8.5. The hydrogen-bonding network created by the protonated phosphonates is believed to provide a catalytic pathway for exchange of the bound water protons with protons of bulk water (56,57). Gd(DOTP)<sup>5-</sup> shows no pH dependence, and has been used to account for concentration of the pH-responsive agent to produce high resolution pH maps of a mouse kidney (58; Figure 11) and rat glioma (56). Water can easily access the Gadolinium ion in Gd-DOTA, but the accessibility is hindered in a tetrameric form of Gd-DOTA. This lower accessibility is modulated by the protonation state of the carboxylate ligands, so that the T1 relaxation time of the Gd-DOTA tetramer becomes pH-dependent (59). Water accessibility can also be changed through acid-catalyzed dissociation of a nitrophenol from gadolinium in Gd(NP-DO3A), while the 'control agent' Gd(NP-DO3AM)

## Responsive MRI contrast agents

**Table 3.** Structures of MR contrast agents responsive to metal ions

Responsive to	Structure	References
Calcium (Ca)		45
Zinc (Zn)		47
Iron (Fe)		48
Iron (Fe)		49
Zinc (Zn)		50

**Table 4.** Structures of MR contrast agents responsive to pH

Responsive to	Structure	References
pH	 <p>Chemical structure of a macrocyclic MR contrast agent. It features a 12-membered ring with four nitrogen atoms. Each nitrogen is part of a side chain containing a phosphate group (<math>\text{H}_2\text{O}_3\text{PCH}_2\text{NH}</math>).</p>	57
pH	 <p>Chemical structure of a macrocyclic MR contrast agent. It features a 12-membered ring with four nitrogen atoms. One nitrogen is substituted with a 3-nitrophenyl group (<math>\text{O}_2\text{N}</math> and <math>\text{OH}</math>).</p>	60
pH	 <p>Chemical structure of a macrocyclic MR contrast agent. It features a 12-membered ring with four nitrogen atoms. The ring is substituted with various groups: <math>\text{R}_1</math>, <math>\text{R}_2</math>, <math>\text{H}</math>, <math>\text{t-Bu}</math>, and <math>\text{OMe}</math>.</p>	61
pH	 <p>Chemical structure of a macrocyclic MR contrast agent. It features a 12-membered ring with four nitrogen atoms. One nitrogen is substituted with a pyridine ring (<math>\text{R}</math>).</p>	63
pH	 <p>Chemical structure of a macrocyclic MR contrast agent. It features a 12-membered ring with four nitrogen atoms. The ring is substituted with a gadolinium ion (<math>\text{Gd}^{3+}</math>).</p>	68
pH	 <p>Chemical structure of a macrocyclic MR contrast agent. It features a 12-membered ring with four nitrogen atoms. The ring is substituted with a long alkyl chain (<math>\text{C}_{18}\text{H}_{37}</math>) and a gadolinium ion (<math>\text{Gd}^{3+}</math>).</p>	69
pH	 <p>Chemical structure of a macrocyclic MR contrast agent. It features a 12-membered ring with four nitrogen atoms. The ring is substituted with a complex side chain containing a carboxylic acid group (<math>\text{HO}</math>), a hydroxyl group (<math>\text{OH}</math>), and a carboxylate group (<math>\text{COO}^-</math>).</p>	73
pH	 <p>Chemical structure of a macrocyclic MR contrast agent. It features a 12-membered ring with four nitrogen atoms. Each nitrogen is part of a side chain containing a carboxylate group (<math>\text{COO}^-</math>).</p>	75

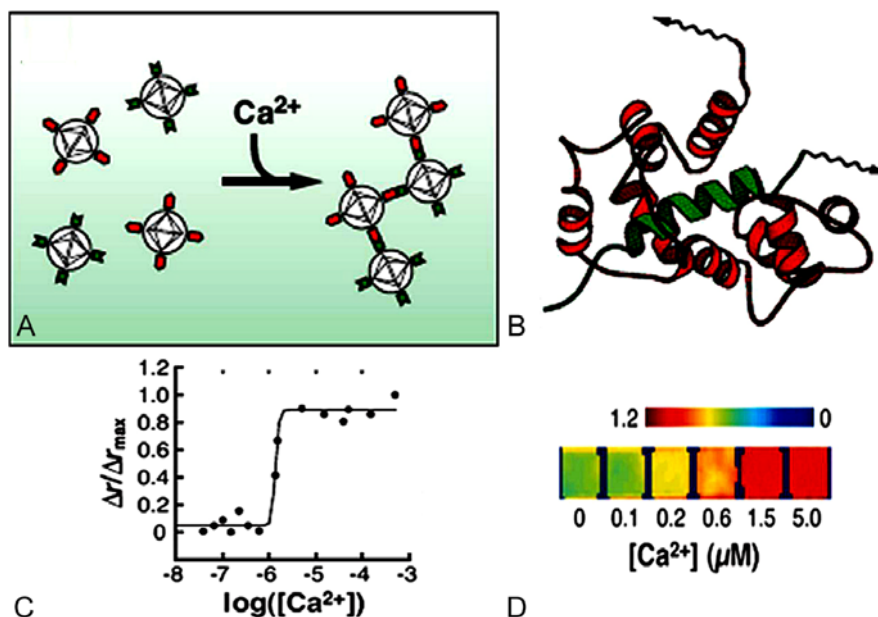


**Figure 10.** An example of a metal-responsive MRI contrast agent that acts as a calcium sensor. (*A and B*) Iron-labeled peptidyl derivatives from calmodulin (red) and M13 (green) form binary aggregates in the presence, but not the absence, of calcium. (*C*) Calcium titrations were performed to determine the EC50 of the calcium sensor. EGTA-buffered solutions were used for 0–1.35 micromolar and 39M  $\text{Ca}^{2+}$  concentrations, and unbuffered calcium solutions were used for the remainder of concentrations in the 1.5–500 micromolar range. The EC50 was  $1.4 \pm 0.1$  micromolar  $\text{Ca}^{2+}$ . (*D*) A normalized MRI image showing relative signal obtained from 7.9 mg/liter 3C:1M sensor in the presence of 0–5.0  $\mu\text{M}$  calcium ions. Reproduced with permission from (52).

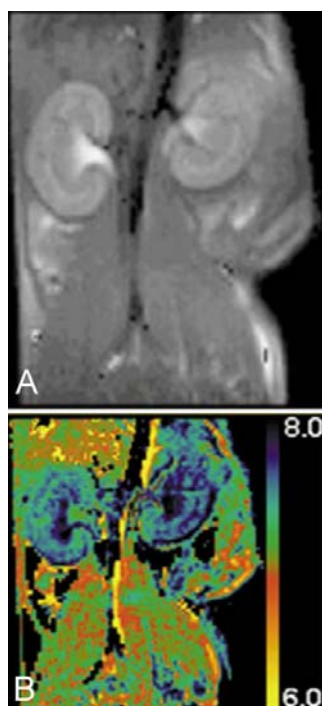


**Figure 11.** An example of a pH-responsive MRI contrast agent. A) A T1-weighted MR image of an acetazolamide-treated mouse was acquired after administering a contrast agent that changes T1 relaxivity in response to pH. B) The parametric map of pH was determined by comparing MR images with pH-responsive and pH-unresponsive MRI contrast agents. The pH-unresponsive agent served as a control to account for in vivo pharmacokinetics, which were assumed to be identical for the agents. Reproduced with permission from (58).





**Figure 12.** An example of a temperature-responsive MRI contrast agent. A phantom containing the agent (1 mL, 10 mM, pH 7.0) was heated with warm air flowing over the sample. The temperature of the air is indicated in each figure, while the temperatures within the sample are shown by the color bar (in units of degrees C). Reproduced with permission from (80).

shows no dissociation and only a modest pH-dependent change in T1 relaxation time (60). A pH-dependent sulfonamide ligation of gadolinium can switch the hydration state of this lanthanide, although the binding of endogenous anions or proteins may also affect the hydration state and suppress the expected pH-dependent change in T1 relaxation time (61,62). Triaquahexaazamacrocyclic complexes experience a reduction of water accessibility due to the coordination with hydroxide anions, which can be exploited to measure basic pH ranges (63). Liposomes consisting of dipalmitoyl phosphatidyl ethanolamine and palmitic acid show pH-dependent stabilities, which can be exploited to cause a change in the water accessibility of T1 contrast agents that are encapsulated in these liposomes (64,65). A cationic polyion complex swells at low pH, which changes the accessibility of water for the contrast agents within the complex (66).

MRI contrast agents can experience a change in rotational tumbling time in response to pH changes. Aggregation of  $Gd_xC60(OH)_x$  or  $Gd_xC60[C(COOH)_2]_{10}$  gadofullerene derivatives occurs at low pH, which causes a decrease in T1 relaxation time as the pH is changed from 12 to 3 (67). High pH causes deprotonation of phospholipid mimetic structures HADO-(Gd-DO3A) and C18<sub>2</sub>-(Gd-DTPA-Glu), which causes higher lipophilicity that drives formation of colloidal aggregates, causing the T1 relaxation time to decrease at higher pH (68,69). A PAMAM dendritic contrast agent exhibits an increase in rigidity as pH decreases from 11 to 6, causing T1 relaxation time to decrease by 60% (70). Self assembled magnetic micelles change hydrodynamic diameter from 200 nm at low pH to 300 nm at high pH, which changes the T2\* relaxation time of iron oxide nanoparticles that are encapsulated within the micelle (71). A polyornithine polymer exhibits a flexible random coil conformation at low pH and forms a rigid helical conformation at high pH, which decreases the T1 relaxation time of gadolinium chelates that are attached to the polymer (72,73).

The base-catalyzed exchange of amide hydrogens and water hydrogens is dependent on pH. MRI contrast agents that contain primary or secondary amide groups have shown large increases in PARACEST with increasing pH (74-77). This approach has been extended to non-paramagnetic polylysine and PAMAM dendrimers that show a pH-dependent CEST effect (78). A pH-

unresponsive PARACEST effect may be generated by a metal-bound water molecule, which provides the opportunity to monitor a pH-responsive and pH-unresponsive PARACEST effect from the same contrast agent (77). The ratio of these two PARACEST effects can provide a concentration-independent measure of pH. A similar ratiometric approach has been applied to the PARACEST effects from the acid-catalyzed hydrogen exchange of an amine group and a base-catalyzed hydrogen exchange of an amide group, which provides a greater dynamic range of PARACEST imaging for measuring pH (Liu, Li and Pagel, unpublished results).

### 5.7. Molecular imaging of temperature

MR thermometry techniques have been developed to address pathologies such as heart arrhythmias (79), and the increasing needs for assessing thermal-based drug delivery and thermal ablation therapies (80). The high spatial resolution and temporal resolution of MRI makes this modality particularly useful for thermal mapping. Ideally, MRI contrast agents that are responsive to changes in temperature must be very accurate and must not be adversely affected by other environmental conditions such as pH or molecular compositions. The temperature dependence of MR frequencies can meet these conditions. For example, PARACEST thermometry has been performed by identifying the MR frequency that provides the greatest PARACEST effect, and these results have been translated to generate a temperature map (81; Figure 12).

The transmembrane permeability of liposomes can be strongly dependent on temperature. Liposomes that encapsulate Gd(DTPA)-BMA show slow water exchange between the liposome interior and exterior, but this water exchange rate shows a sharp increase as the temperature exceeds the gel-to-liquid crystalline phase-transition temperature of the liposomes (82). Similarly, the exchange of gadolinium- or manganese-containing MRI contrast agents can more easily escape the interior of the liposomes above the phase-transition temperature (83). In both cases, the increased water accessibility to the agent leads to a decreased T1 relaxation time.

## 6. FUTURE DIRECTIONS

The dawning of the field of responsive MRI contrast agents has necessarily required extensive designs and characterizations of unique MRI contrast agents in order to creatively explore the relationships between molecular responses and changes in MRI contrast agents. This approach has often required the development of specialized synthetic schemes to produce each unique MRI contrast agent. These explorations of specialized contrast agents have been necessarily ponderous, resulting in only 52 examples during the last 10 years. To accelerate the application of responsive MRI contrast agents, a greater focus should be placed on agents that can be rapidly synthesized with high yield and purity, and that can be applied to large sets of molecular biomarkers. For example, T2\* agents that are depolymerized by an enzyme can be rapidly synthesized by linking iron oxide nanoparticles with peptide linkers. Similarly, the synthesis



of a PARACEST agent with a peptidyl ligand can be accomplished with a commercially available solid phase peptide synthesizer (84). In both cases, the sequence of the peptide ligand can be chosen to be sensitive to one of many protease enzymes, so that each of these types of responsive MRI contrast agents can be easily applied to detect specific members of the human proteome (85).

Because pathologies often exhibit modest changes in the expression, production, delivery, or activity of various biomarkers, an emphasis should be placed on the ability to quantitatively translate the response in MR image contrast to the concentration of the biomarker. Absolute quantifications of MR image contrast is a daunting challenge, because many characteristics of the sample or patient, the instrumentation, and the choice of acquisition parameters and image processing methods can alter image contrast. Ratiometric quantifications are more feasible, in which the response caused by a molecular biomarker is the only effect that is allowed to vary between two MR images, or between two or more regions of the same image. PARACEST may greatly facilitate ratiometric quantifications, because two or more PARACEST agents can be selectively detected within the same sample volume by saturating their respective CEST MR frequencies. The selective detection of each PARACEST agent also provides opportunities to detect more than one molecular target during a single MRI scan session, which may lead to the diagnoses of “molecular signatures”, or multiple molecular biomarkers of pathological tissues.

In most examples, the direct interaction of a responsive MRI contrast agent and a molecular biomarker has directly led to a change in MRI contrast. Some recent examples demonstrate that more complex mechanisms in molecular biology can be cleverly incorporated to form multi-step processes that indirectly link the interaction of responsive MRI contrast agents and biomarkers with an eventual change in MRI contrast. Reporter gene imaging is an obvious example, in which the steps of gene transcription and translation to form a reporter protein, the delivery of an agent to the target tissue (and possibly to the target cell, target intracellular environment and intracellular organelle), and the interaction of the agent and reporter protein must each occur before MRI contrast is altered. Additional multi-step mechanisms such as post-translational protein processing, protein-protein interactions, and cell-cell signaling are likely to be employed with future responsive MRI contrast agents. Therefore, interdisciplinary research that combines molecular biology with radiology and chemistry will be critical for further developing responsive MRI contrast agents. This review provides a single-step foundation for developing these multi-step mechanisms that can expand the armamentarium of molecular imaging for detecting molecular biomarkers of many pathologies.

## 7. ACKNOWLEDGEMENTS

The authors would like to thank Guanshu Liu and Dr. Yuguo Li, Case Western Reserve University, for

contributions of unpublished research. This work was facilitated by the Northeastern Ohio Animal Imaging Resource Center, an NIH funded program #R24CA110943, part of the Case Center for Imaging Research. Byunghye Yoo's efforts are supported by a fellowship from the Biomedical Research Technology Transfer program of the state of Ohio.

## 8. REFERENCES

1. 2006 MRI Market Summary Report. IMV International Des Plaines, Ill. (2007)
2. Bluemke D, C. Gatsonis, M. H. Chen, G. A. DeAngelis, N. DeBruhl, S. Harms, S. H. Heywang-Koebrunner, N. Hylton, C. K. Kuhl, C. Lehman, E. D. Pisano, P. Causer, S. J. Schnitt, S. F. Smazal, C. B. Stelling, P. T. Weatherall, M. D. Schnall: Magnetic resonance imaging of the breast prior to biopsy. *J Am Med Assoc* 292, 2735-2742 (2004)
3. Schott A, M. A. Roubidoux, M. A., Helvie, D. F. Hayes, C. G. Kleer, L. A. Newman, L. J. Pierce, K. A. Griffith, S. Murray, K. A. Hunt, C. Paramagul, L. H. Baker: Clinical and Radiologic Assessments to Predict Breast Cancer Pathologic Complete Response to Neoadjuvant Chemotherapy. *Breast Cancer Research and Treatment*, 92, 231-238 (2005)
4. Martens L, H. Hermjakob, P. Jones, C. Taylor, K. Gevaert, J. Vandekerckhove, R. Apweiler: PRIDE: The PRoteomics IDentifications database. *Proteomics* 5, 3537-3545 (2005)
5. Jones P, C. Brooksbank: A Quick Guide to PRIDE: The PRoteomics IDentifications Database. *OBBeC Life Science and Bioinformatics* 24-26 (2006)
6. Alves F, P. Donato, A. D. Sherry, A. Zaheer, S. Zhang, A. J. M. Lubag, M. Merritt, R. E. Lenkinski, J. V. Frangioni, M. Neves, M. I. M. Prata, A. C. Santos, L. J. P. de Lama, C. F. G. C. Geraldles: Silencing of Phosphonate-Gadolinium Magnetic Resonance Imaging Contrast by Hydroxyapatite Binding. *Investigative Radiology* 38, 750-760 (2003)
7. Mishra A, J. Pfeuffer, R. Mishra, J. Engelmann, A. K. Mishra, K. Ugurbil, N. K. Logothetis: A new class of Gd-based DO3A-ethylamine-derived targeted contrast agents for MR and optical imaging. *Bioconjugate Chem* 17, 773-780 (2006)
8. Caravan P, N. J. Cloutier, M. T. Greenfield, S. A. McDermid, S. U. Dunham, J. W. M. Bulte, J. C. Amedio, R. J. Looby, R. M. Supkowski, W. D. Horrocks, T. J. McMurphy, R. B. Lauffer: The interaction of MS-325 with human serum albumin and its effect on proton relaxation rates. *J Am Chem Soc* 124, 3152-3162 (2002)
9. De Leon-Rodriguez L, A. Ortiz, A. L. Weiner, S. Zhang, Z. Kovacs, T. Kodadek, A. D. Sherry: Magnetic resonance imaging detects a specific peptide-protein binding event. *J Am Chem Soc* 124, 3514-3515 (2002)
10. Anelli P, I. Bertini, M. Fragai, L. Lattuada, C. Luchinat, G. Parigi: Sulfonamide-functionalized gadolinium DTPA complexes as possible contrast agents for MRI: A relaxometric investigation. *Euro J Inorg Chem* 4, 625-630 (2000)
11. Artemov D: Molecular magnetic resonance imaging with targeted contrast agents. *J Cell Biol* 90, 518-524 (2003)

12. Louie A, H. M. Huber, E. T. Ahrens, U. Rothbacher, R. Moats, R. E. Jacobs, S. E. Fraser, T. J. Meade: *In vivo* visualization of gene expression using magnetic resonance imaging. *Nature Biotechnol* 18, 321-325 (2000)
13. Yoo B, M. D. Pagel: A PARACEST MRI contrast agent to detect enzyme activity. *J Am Chem Soc* 128, 14302-14303 (2006)
14. Lauffer R, T. J. McMurry, S. O. Dunham, D. M. Scott, D. J. Parmelee, S. Dumas: Bioactivated diagnostic imaging contrast agents. WIPO Patent Application 97/36619 (1997)
15. Nivorozhkin A, A. F. Kolodziej, P. Caraban, M. T. Greenfield, R. B. Lauffer, T. J. McMurry: Enzyme activated Gd<sup>3+</sup> magnetic resonance imaging contrast agents with a prominent receptor induced magnetization enhancement. *Angew Chem Int Ed* 40, 2903-2906 (2001)
16. Bogdanov A, L. Matuszewski, C. Bremer, A. Petrovski, R. Weissleder: Oligomerization of paramagnetic substrates result in signal amplification and can be used for MR imaging of molecular targets. *Molecular Imaging* 1, 16-23 (2002)
17. Chen J, W. Pham, R. Weissleder, A. Bogdanov: Human myeloperoxidase: a potential target for molecular MR imaging in atherosclerosis. *Magn Reson Med* 52, 1021-1028 (2004)
18. Chen J, M. Querol, A. Bogdanov, R. Weissleder: Imaging myeloperoxidase in mice by using novel amplifiable paramagnetic substrates. *Radiology* 240, 473-481 (2006)
19. Querol M, J. W. Chen, R. Weissleder, A. Bogdanov: DTPA-bisamide-based MR sensor agents for peroxidase imaging. *Org Lett* 7, 1719-1722 (2005)
20. Querol M, J. W. Chen, A. Bogdanov: A paramagnetic contrast agent with myeloperoxidase-sensing properties. *Org Biomol Chem* 4, 1887-1895 (2006)
21. Aime S, C. Cabella, S. Colombatto, S. G. Crich, E. Gianolio, F. Maggioni: Insight into the use of paramagnetic Gd(III) complexes in MR molecular imaging investigations. *J Magn Reson Imaging* 16, 394-406 (2002)
22. Duimstra J, T. J. Meade: Self-immolative magnetic resonance imaging contrast agents sensitive to beta-glucuronidase. WIPO Patent Application 05/115105 (2005)
23. Shiftan L, T. Israely, M. Cohen, V. Frydman, H. Dafni, R. Stern, M. Neeman: Magnetic resonance imaging visualization of hyaluronidase in ovarian carcinoma. *Cancer Res* 65, 10316-10323 (2005)
24. Shiftan L, M. Neeman: Kinetic analysis of hyaluronidase activity using a bioactive MRI contrast agent. *Contrast Media & Molecular Imaging* 1, 106-112 (2006)
25. Perez J, F. J. Simeone, A. Tsourkas, L. Josephson, R. Weissleder: Peroxidase substrate nanosensors for MR imaging. *Nanoletters* 4, 119-122 (2004)
26. Perez J, L. Josephson, T. O'Loughlin, D. Hogemann, R. Weissleder: Magnetic relaxation switches capable of sensing molecular interactions. *Nature Biotechnol* 20, 816-820 (2002)
27. Zhao M, L. Josephson, Y. Tang, R. Weissleder: Magnetic sensors for protease assays. *Angew Chem Int Ed* 43, 1375-1378 (2003)
28. Perez J, T. O'Loughlin, F.J. Simeone, R. Weissleder, L. Josephson: DNA-based magnetic nanoparticle assembly acts as a magnetic relaxation nanoswitch allowing screening of DNA-cleaving agents. *J Am Chem Soc* 124, 2856-1857 (2002)
29. Lander E, L. M. Linton, B. Birren, C. Nusbaum, M. C. Zody: Initial sequencing and analysis of the human genome. *Nature* 409, 860-921 (2001)
30. Venter J, M. D. Adams, E. W. Myers, P. W. Li, R. J. Mural, G. G. Sutton, H. O. Smith, M. Yandell, C. A. Evans, R. A. Holt, J. D. Gocayne, P. Amanatides, R. M. Ballew, D. H. Huson, J. Russo Wortman, Q. Zhang, C. D. Kodira, X. H. Zheng, L. Chen, M. Skupski, G. Subramanian, P. D. Thomas, J. Zhang, G. L. G. Miklos, C. Nelson, S. Broder, A. G. Clark, J. Nadeau, V. A. McKusick, N. Zinder, A. J. Levine, R. J. Roberts, M. Simon, C. Slayman, M. Hunkapiller, R. Bolanos, A. Delcher, I. Dew, D. Fasulo, M. Flanigan, L. Florea, A. Halpern, S. Hannenhalli, S. Kravitz, S. Levy, C. Mobarry, K. Reinert, K. Remington, J. Abu-Threideh, E. Beasley, K. Biddick, V. Bonazzi, R. Brandon, M. Cargill, I. Chandramouliswaran, R. Charlab, K. Chaturvedi, Z. Deng, V. Di Francesco, P. Dunn, K. Eilbeck, C. Evangelista, A. E. Gabrielian, W. Gan, W. Ge, F. Gong, Z. Gu, P. Guan, T. J. Heiman, M. E. Higgins, R.-R. Ji, Z. Ke, K. A. Ketchum, Z. Lai, Y. Lei, Z. Li, J. Li, Y. Liang, X. Lin, F. Lu, G. V. Merkulov, N. Milshina, H. M. Moore, A. K. Naik, V. A. Narayan, B. Neelam, D. Nusskern, D. B. Rusch, S. Salzberg, W. Shao, B. Shue, J. Sun, Z. Y. Wang, A. Wang, X. Wang, J. Wang, M.-H. Wei, R. Wides, C. Xiao, C. Yan, A. Yao, J. Ye, M. Zhan, W. Zhang, H. Zhang, Q. Zhao, L. Zheng, F. Zhong, W. Zhong, S. C. Zhu, S. Zhao, D. Gilbert, S. Baumhueter, G. Spier, C. Carter, A. Cravchik, T. Woodage, F. Ali, H. An, A. Awe, D. Baldwin, H. Baden, M. Barnstead, I. Barrow, K. Beeson, D. Busam, A. Carver, A. Center, M. L. Cheng, L. Curry, S. Danaher, L. Davenport, R. Desilets, S. Dietz, K. Dodson, L. Doup, S. Ferriera, N. Garg, A. Gluecksmann, B. Hart, J. Haynes, C. Haynes, C. Heiner, S. Hladun, D. Hostin, J. Houck, T. Howland, C. Ibegwam, J. Johnson, F. Kalush, L. Kline, S. Koduru, A. Love, F. Mann, D. May, S. McCawley, T. McIntosh, I. McMullen, M. Moy, L. Moy, B. Murphy, K. Nelson, C. Pfannkoch, E. Pratts, V. Puri, H. Qureshi, M. Reardon, R. Rodriguez, Y.-H. Rogers, D. Romblad, B. Ruhfel, R. Scott, C. Sitter, M. Smallwood, E. Stewart, R. Strong, E. Suh, R. Thomas, N. N. Tint, S. Tse, C. Vech, G. Wang, J. Wetter, S. Williams, M. Williams, S. Windsor, E. Winn-Deen, K. Wolfe, J. Zaveri, K. Zaveri, J. F. Abril, R. Guigó, M. J. Campbell, K. V. Sjolander, B. Karlak, A. Kejariwal, H. Mi, B. Lazareva, T. Hatton, A. Narechania, K. Diemer, A. Muruganujan, N. Guo, S. Sato, V. Bafna, S. Istrail, R. Lippert, R. Schwartz, B. Walenz, S. Yooseph, D. Allen, A. Basu, J. Baxendale, L. Blick, M. Caminha, J. Carnes-Stine, P. Caulk, Y.-H. Chiang, M. Coyne, C. Dahlke, A. Deslattes Mays, M. Dombroski, M. Donnelly, D. Ely, S. Esparham, C. Fosler, H. Gire, S. Glanowski, K. Glasser, A. Glodek, M. Gorokhov, K. Graham, B. Gropman, M. Harris, J. Heil, S. Henderson, J. Hoover, D. Jennings, C. Jordan, J. Jordan, J. Kasha, L. Kagan, C. Kraft, A. Levitsky, M. Lewis, X. Liu, J. Lopez, D. Ma, W. Majoros, J. McDaniel, S. Murphy, M. Newman, T. Nguyen, N. Nguyen, M. Nodell, S. Pan, J. Peck, M. Peterson, W. Rowe, R. Sanders, J. Scott, M. Simpson, T. Smith, A. Sprague, T. Stockwell, R. Turner, E. Venter, M. Wang, M. Wen, D. Wu, M. Wu, A. Xia, A. Zandieh, X. Zhu: The sequence of the human genome. *Science* 291, 1304-1351 (2001)

31. Caravan P, J. M. Greenwood, J. T. Welch, S. J. Franklin: Gadolinium-binding helix-turn-helix peptides: DNA-dependent MRI contrast agents. *Chem Commun* 2574-2575 (2003)
32. Bremer C, R. Weissleder: *In vivo* imaging of gene expression: MR and optical technologies. *Acad Radiol* 8, 15-23 (2001)
33. Hogemann D, J.P. Basilion: "Seeing inside the body": MR imaging of gene expression. *Eur J Nucl Med* 29, 400-408 (2002)
34. Zhang S, R. Trokowski, A. D. Sherry: A Paramagnetic CEST Agent for Imaging Glucose by MRI. *J Am Chem Soc* 125(50), 15288-15289 (2003)
35. Trokowski R, S. Zhang, A. D. Sherry: Cyclen-Based Phenylboronate Ligands and Their Eu<sup>3+</sup> Complexes for Sensing Glucose by MRI. *Bioconjugate Chem* 15, 1431-1440 (2004)
36. Aime S, D. D. Castelli, F. Fedeli, E. Terreno: A paramagnetic MRI-CEST agent responsive to lactate concentration. *J Am Chem Soc* 124, 9364-9365 (2002).
37. Rohovec J, T. Maschmeyer, S. Aime, J. A. Peters: The structure of the sugar residue in glycated human serum albumin and its molecular recognition by phenylboronate. *Chem Eur J* 9, 2193-2199 (2003)
38. Glogard C, G. Stensrud, S. Aime: Novel radical-responsive MRI contrast agent based on paramagnetic liposomes. *Magn Reson Chem* 41(8), 585-588 (2003)
39. Powers W, R. L. Grubb, Jr., D. Darriet, M. E. Raichle: Cerebral blood flow and cerebral metabolic rate of oxygen requirements for cerebral function and variability in humans. *J Cereb Blood Flow Metab* 5, 600-608 (1985)
40. Mason R, S. Ran, P. E. Thorpe: Quantitative assessment of tumor oxygen dynamics: Molecular imaging for prognostic radiology. *J Cell Biochem Suppl* 87, 45-53 (2002)
41. Aime S, M. Botta, E. Gianolio, E. Terreno: A p(O<sub>2</sub>)-responsive MRI contrast agent based on the redox switch of manganese(II/III)-porphyrin complexes. *Angew Chem Int Ed* 39, 747-750 (2000)
42. Sun P, Z. B. Schoening, A. Jasanoff: *In vivo* oxygen detection using exogenous hemoglobin as a contrast agent in magnetic resonance spectroscopy. *Magn Reson Med* 49, 609-614 (2003)
43. Aime S, G. Digilio, M. Fasano, S. Paoletti, A. Arnelli, P. Ascenzi: Metal complexes as allosteric effectors of human hemoglobin: An NMR study of the interaction of the Gadolinium(III) Bis(*m*-boroxyphenylamide)diethylenetriaminepentaacetic acid complex with human oxygenated and deoxygenated hemoglobin. *Biophys J* 76, 2735-2743 (1999)
44. Li W-H, S. E. Fraser, T. J. Meade: A calcium-sensitive magnetic resonance imaging contrast agent. *J Am Chem Soc* 121, 1413-1414 (1999)
45. Li W-H, G. Parigi, M. Fragai, C. Luchinat, T. J. Meade: Mechanistic studies of a calcium-dependent MRI contrast agent. *Inorg Chem* 41, 4018-4024 (2002)
46. Hanaoka K, K. Kikuchi, Y. Urano, T. Nagano: Selective sensing of zinc ions with a novel magnetic resonance imaging contrast agent. *J Chem Soc Perkin Trans 2* 9, 1840-1843 (2001)
47. Hanaoka K, K. Kikuchi, Y. Urano, M. Narazaki, T. Yokawa, S. Sakamoto, K. Yamaguchi, T. Nagano: Design and synthesis of a novel magnetic resonance imaging contrast agent for selective sensing of zinc ion. *Chem Biol* 9, 1027-1032 (2002)
48. Comblin V, D. Gilsoul, M. Hermann, V. Humblet, V. Jacques, M. Mesbahi, C. Sauvage, J. F. Desreux: Designing new MRI contrast agents: a coordination chemistry challenge. *Coord Chem Rev* 185-186, 451-470 (1999)
49. Costa J, R. Ruloff, L. Burai, L. Helm, A. E. Merbach: Rigid MIL2Gd2III (M = Fe, Ru) Complexes of a Terpyridine-Based Heteroditopic Chelate: A Class of Candidates for MRI Contrast Agents. *J Am Chem Soc* 127, 5147-5157 (2005)
50. Livramento J, E. Toth, A. Sour, A. Borel, A. E. Merbach, R. Ruloff: High relaxivity confined to a small molecular space: a metallostar-based, potential MRI contrast agent. *Angew Chem Int Ed* 44, 1480-1484 (2005)
51. Trokowski R, J. Ren, F. K. Kalman, A. D. Sherry: Selective sensing of zinc ions with a PARACEST contrast agent. *Angew Chem Int Ed* 44, 6920-6923 (2005)
52. Atanasijevic T, M. Shusteff, P. Fam, A. Jasanoff: Calcium-sensitive MRI contrast agents based on superparamagnetic iron oxide nanoparticles and calmodulin. *Proc Natl Acad Sci USA* 103, 14707-14712 (2006)
53. Adroque H, N. E. Madias: Management of life-threatening acid-base disorders. *New England J Med* 338, 26-34 (1998)
54. Gatenby R, R. J. Gillies: Why do cancers have high aerobic glycolysis? *Nature Reviews Cancer* 4, 891-899 (2004)
55. Garcia-Martin M, G. V. Martinez, M. Raghunand, A. D. Sherry, S. Zhang, R. J. Gillies: High-resolution pH imaging of rat glioma using pH-dependent relaxivity. *Magn Reson Med* 55, 309-315 (2006)
56. M. Raghunand, S. Zhang, A. D. Sherry, R. J. Gillies: *In vivo* magnetic resonance imaging of tissue pH using a novel pH-sensitive contrast agent, GdDOTP-4Amp. *Acad Radiology* 9 suppl2, S481-S483 (2002)
57. Zhang S, L. Michaudet, S. Burgess, A. D. Sherry: A novel pH-responsive MRI contrast agent. *Angew Chem Int Ed* 38, 3192-3194 (1999)
58. Raghunand N, C. Howison, A. D. Sherry, S. Zhang, R. J. Gillies: Renal and systemic pH imaging by contrast-enhanced MRI. *Magn Reson Med* 49, 249-257 (2003)
59. Jebasingh B, V. Alexander: Synthesis and relaxivity studies of a tetranuclear gadolinium(III) complex of DO3A as a contrast-enhancing agent for MRI. *Inorg Chem* 44, 9434-9443 (2005)
60. Woods M, G. E. Kiefer, S. Bott, A. Castillo-Muzquiz, C. Eshelbrenner, L. Michaudet, K. McMillan, S. D. K. Mudigunda, D. Ogrin, G. Tircso, S. Zhang, P. Zhao, A. D. Sherry: Synthesis, relaxometric and photophysical properties of a new pH-responsive MRI contrast agent: The effect of other ligating groups on dissociation of a p-Nitrophenolic pendant arm. *J Am Chem Soc* 126, 9248-9256 (2004)
61. Lowe M, D. Parker, O. Reany, S. Aime, M. Botta, G. Castellano, E. Gianolio, R. Pagliarin: pH-dependent modulation of relaxivity and luminescence in macrocyclic gadolinium and europium complexes based on reversible intramolecular sulfonamide ligation. *J Am Chem Soc* 123, 7601-7609 (2001)

62. Woods M, S. Zhang, V. H. Ebron, A. D. Sherry: pH-sensitive modulation of the second hydration sphere in lanthanide(III) tetraamide-DOTA complexes; a novel approach to smart MR contrast media. *Chemistry* 9, 4634-4640 (2003)
63. Hall J, R. Haner, S. Aime, M. Botta, S. Faulker, D. Parker, A. S. de Sousa: Relaxometric and luminescence behavior of triaqua-hexaazamacrocyclic complexes displaying a high relaxivity with a pronounced pH dependence. *New J Chem* 22, 627-631 (1998)
64. Lokling K, S. L. Fossheim, R. Skurtveit, A. Bjornerud, J. Klaveness: pH-sensitive paramagnetic liposomes as MRI contrast agents: *in vitro* feasibility studies. *Magn Reson Imaging* 19, 731-738 (2001)
65. Lokling K, R. Skurtveit, S. L. Fossheim, G. Smistad, I. Henrikson, J. Klaveness: pH-Sensitive paramagnetic liposomes for MRI: assessment of stability in blood. *Magn Reson Imaging* 21, 531-540 (2003)
66. Mikawa M, N. Miwa, M. Bratigam, T. Akaike, A. Maruyama: Gd<sup>3+</sup>-loaded polyion complex for pH detection with magnetic resonance imaging. *J Biomed Mater Res* 49, 390-395 (2000)
67. Toth E, R.D. Bolskar, A. Borel, G. Gonzales, L. Helm, A. E. Merbach, B. Sitharaman, L. J. Wilson: Water-soluble gadofullerenes: Toward high-relaxivity, pH-responsive MRI contrast agents. *J Am Chem Soc* 127, 799-805 (2005)
68. Hovland R, C. Glogard, A. J. Aasen, J. Klaveness: Gadolinium DO3A derivatives mimicking phospholipids; preparation and *in vitro* evaluation as pH responsive MRI contrast agents. *J Chem Soc Perkin Trans 2* 6, 929-933 (2001)
69. Vaccaro M, A. Accardo, D. Tesaro, G. Mangiapia, D. Lof, K. Schillen, O. Soderman, G. Morelli, L. Paduano: Supramolecular aggregates of amphiphilic gadolinium complexes as blood pool MRI/MRA contrast agents: physicochemical characterization. *Langmuir* 22, 6635-6643 (2006)
70. Laus S, A. Sour, R. Ruloff, E. Toth, A. E. Merbach: Rotational dynamics account for pH-dependent relaxivities of PAMAM dendrimeric, Gd-based potential MRI contrast agents. *Chemistry-A European Journal* 11, 3064-3076 (2005)
71. Lecommandoux S, O. Sandre, F. Checot, R. Perzynski: Smart hybrid magnetic self-assembled micelles and hollow capsules. *Progress in Solid State Chemistry* 34, 171-179 (2006)
72. Aime S, M. Botta, S. M. Crich, G. Giovenzan, G. Palmisano, M. Sisti: A macromolecular Gd(III) complex as pH-responsive relaxometric probe for MRI applications. *Chem Commun* 16, 1577-1578 (1999).
73. Aime S, M. Botta, S. G. Crich, G. Giovenzana, G., Palmisano, M. Sisti: Novel Paramagnetic Macromolecular Complexes Derived from the Linkage of a Macrocyclic Gd(III) Complex to Polyamino Acids through a Squaric Acid Moiety. *Bioconjugate Chem* 10, 192-199 (1999)
74. Aime S, A. Barge, D. D. Castelli, F. Fedeli, A. Mortillaro, F. U. Nielsen, E. Terreno: Paramagnetic lanthanide(III) complexes as pH-sensitive chemical exchange saturation transfer (CEST) contrast agents for MRI applications. *Magn Reson Med* 47, 639-648 (2002)
75. Aime S, D. D. Castelli, E. Terreno: Novel-pH reporter MRI contrast agents. *Angew Chem Int Ed* 41, 4334-4336 (2002).
76. Zhang S, L. Michaudet, S. Burgess, A. D. Sherry: The amide protons of an Ytterbium(III) dota tetraamidecomplex as efficient antennae for transfer of magnetization to bulk water. *Angew Chem Int Ed* 114, 1999-2001 (2002)
77. Terreno E, D. D. Castelli, G. Cravotto, L. Milone, S. Aime: Ln(III)DOTAMGly complexes: a versatile series to assess the determinants of the efficiency of paramagnetic chemical exchange saturation transfer agent for magnetic resonance imaging applications. *Investigative Radiology* 39, 235-243 (2004)
78. van Zijl P, J. H. Duyn, L. H. Bryant, J. W. M. Bulte: The use of starburst dendrimers as pH contrast agents. *Proc Int Soc Magn Reson Med* 9, 878 (2003)
79. Levy S: Biophysical basis and cardiac lesions caused by different techniques of cardiac arrhythmia ablation. *Arch Mal Coeur Vaiss* 88, 1465-1469 (1995)
80. Weidensteiner C, B. Quesson, B. Caire-Gana, N. Keroui, A. Rullier, H. Trillaud, C. T. W. Moonen: Real-time MR temperature mapping of rabbit liver *in vivo* during thermal ablation. *Magn Reson Med* 50, 322-330 (2003)
81. Zhang S, C. R. Malloy, A. D. Sherry: MRI thermometry based on PARACEST agents. *J Am Chem Soc* 127, 17572-17573 (2005)
82. Fossheim S, K. A. Il'yasov, J. Hennig, A. Bjornerud: Thermosensitive paramagnetic liposomes for temperature control during MR imaging-guided hyperthermia: *in vitro* feasibility studies. *Acad Radiol* 7, 1107-1115 (2000)
83. Lindner L, H. M. Reinl, M. Schlemmer, R. Stahl, M. Peller: Paramagnetic thermosensitive liposomes for MR-thermometry. *Int J Hyperthermia* 21, 575-588 (2005)
84. Yoo B, M. D. Pagel: Peptidyl Molecular Imaging Contrast Agents Using a New Solid-Phase Peptide Synthesis Approach. *Bioconjugate Chem* 18, 903-911 (2007)
85. Lopez-Otin C, C.M. Overall: Protease degradomics: a new challenge for proteomics. *Nat Rev Mol Cell Biol* 3, 509-519 (2002)

**Abbreviations:** BMA: bismethylamide; DO3A: 1,4,7,10-tetraazacyclododecane-1,4,7-tetraacetic acid; DOTA: 1,4,7,10-tetraazacyclododecane-1,4,7,10-tetraacetic acid; DOTAM-Gly: 1,4,7,10-tetraazacyclododecane-1,4,7,10-acetic acid tetraglycineamide; DOTP: 1,4,7,10-tetraazacyclododecane-1,4,7,10-tetrakis-(methylenephosphonic acid); DTPA: diethylene-triamine pentaacetic acid; HSA: human serum albumin; MMP: matrix metalloproteinase; MRI: magnetic resonance imaging; NMR: nuclear magnetic resonance; PAMAM: poly(amidoamine); PARACEST: paramagnetic chemical exchange saturation transfer; R<sub>1</sub>: longitudinal (spin-lattice) relaxation time (1/T<sub>1</sub>); R<sub>2</sub>: transverse (spin-spin) relaxation rate (1/T<sub>2</sub>); T<sub>1</sub>: longitudinal (spin-lattice) relaxation time; T<sub>2</sub>: transverse (spin-spin) relaxation time

**Key Words:** Molecular imaging, MRI, Responsive contrast agents, Relaxivity, PARACEST, Review

## **Responsive MRI contrast agents**

**Send correspondence to:** Mark D. Pagel, Ph.D., Case Center for Imaging Research. Departments of Biomedical Engineering, Radiology, and Macromolecular Science and Engineering. Case Western Reserve University, 10900 Euclid Avenue, Cleveland, OHIO, Tel: 216-368-8519, Fax: 216-368-4969, E-mail: [mpagel@case.edu](mailto:mpagel@case.edu)

<http://www.bioscience.org/current/vol13.htm>